Cost analysis of sand barriers in desertified regions based on the land grid division model

YANG Suchang, QU Zhun[*]

School of Economics, Lanzhou University, Lanzhou 730000, China

Abstract: Sand barriers are the most widely used mechanical implements for wind-blown sand control and desertification prevention. However, there is no standard quantitative cost analysis of the sizes and materials required for sand barriers. In this study, based on the original land grid division model for optimal resource utilization, we calculated the total side lengths of square and regular hexagonal sand barriers with the sizes of 1.0 m×1.0 m, 2.0 m×2.0 m, and 3.0 m×3.0 m in a desertified region of the Shapotou area on the southeastern edge of the Tengger Desert, China. Then, through literature review and social survey, we obtained the material cost and material utilization amount of sand barriers with different materials and sizes. Finally, we calculated the costs of square and regular hexagonal sand barriers comprised of wheat straw, corn stalk, *Salix mongolica*, poly lactic acid, magnesium cement, and high-density polyethylene, with the sizes of 1.0 m×1.0 m, 2.0 m×2.0 m, and 3.0 m×3.0 m. The results show that the material cost of regular hexagonal corn stalk sand barriers with the size of 3.0 m×3.0 m is the lowest, while the material cost of square magnesium cement sand barriers with the size of 1.0 m×1.0 m is the highest. When using the same material, the cost of regular hexagonal sand barriers is lower than that of square sand barriers with the same size. When using the same size, the cost of sand barriers with corn stalk material is lower than that of sand barriers with other materials. Based on the above analysis, we can conclude that the economic benefits of regular hexagonal sand barriers are greater than those of square sand barriers. This study provides a theoretical basis for accurately calculating the material cost of sand barriers, particularly for the estimated cost of mechanized sand barrier engineering projects.

Keywords: desertification; corn stalk sand barrier; *Salix mongolica*; land grid division; economic cost; railway; Shapotou area

1 Introduction

Nowadays, the increasingly severe desertification has caused a series of problems, including resource insecurity, poverty, and ecological environmental deterioration, on a global scale (Jing et al., 2022). Although desertified land area in China has been decreasing continuously since the dawn of the 21st century, the prevention and control of desertification is still a matter of concern (Ding et al., 2004; Li et al., 2021). According to the data from the National Forestry and Grassland Administration (2015), the total area of desertified land in China was 1.72×10^8 km^2 in 2015, with 3.00×10^5 km^2 (1.80×10^5 km^2 in arid areas) that has not been effectively controlled. At the current governance rate of 1980.00 km^2/a in China, it will take 152 a to control all the desertified land. It was estimated that 14% of the desertification control work will be completed

by 2035, but only 24% of the total work can be completed until the year 2050 (Yang, 2021). Desertification control is becoming increasingly difficult and prone to relapse, and consolidation and restoration tasks will be heavy in the coming years.

The most successful and widely used sand control measure is the use of square straw sand barriers, also called straw checkerboards. According to Wu (2010), as early as in the 1950s, a Russian expert on sand control has suggested using local wheat grass to make semi-concealed wheat grass sand barriers in Zhongwei County, China on the basis of the experience of setting semi-concealed reed sand barriers in the Caspian Sea Railway. The experimental test in the Shapotou area section along the Baotou-Lanzhou Railway in the Tengger Desert of China has achieved remarkable sand fixation success. For more than 60 a, people have been using checked artificial straw sand barriers there. The implementation of low cost, environmentally friendly artificial straw sand barrier is considered the most effective method of desertification control in China, as well as the rest of the world. The semi-concealed checked artificial straw sand barrier is a type of sand control technology with the most pronounced sand control effect, lowest cost, and most convenient construction (Xu and Xu, 1996; Wang et al., 2009). The reason for this is that owing to the influences of wind, water shortages, sand burying, and other factors, natural vegetation struggles to stably adapt their root system and grow on mobile sand dunes (Liu et al., 2021a), but sand barriers can promote soil crusting and create favorable conditions for plant growth (Lu et al., 2020). The setting of sand barriers can increase surface roughness, thus increasing the starting speed of sand particles, decreasing wind speed and sand transport intensity (Wang, 2018), reducing evaporation, and improving the water content of the sand layer (Wang et al., 2019).

The sand fixation effect of grassy sand barriers is related to the ratio of exposed grass head height and side length (Ling, 1980). The sand-drift transition rate is positively correlated with the height of checkerboard sand barriers and negatively correlated with the spacing of checkerboard sand barriers (Zhu et al., 1998). Wang et al. (2002) and Jiang et al. (2020) stated that the checkerboard sand barrier with the size of 1.0 m×1.0 m is optimal for the sand fixation effect. Several studies and practices (e.g., Zhang et al., 2009; Cheng et al., 2014) have been carried out on wind prevention, sand fixation, ecological impact, and vegetation restoration of sand barriers. However, little is known about the material cost of sand barriers under different grid division standards, and the design of sand fixation engineering lacks an accurate theoretical calculation formula for material consumption. Different material choices and environments lead to the costs of sand control and fixation projects varying greatly in different regions. Wang (2012) took the sand control engineering projects of the Baotou-Lanzhou Railway, the railway in the south of Xinjiang Uygur Autonomous Region, and the Qinghai-Tibet Railway in China as examples, and stated that (1) for the Baotou-Lanzhou Railway, builders lay straw squares on a large area and used corn stalk, branch, bamboo cobs, wood, soil net, and old rope to set up vertical fences to hold back sand, and the sand prevention project costed approximately $2.60×10^6$ CNY/km; (2) the sand prevention engineering project of the section in the railway of the south of Xinjiang primarily adopted reed square, geonet fence, and sand retaining ditch, and the prevention engineering investment ranged from $0.49×10^6$ to $1.45×10^6$ CNY/km; and (3) sand prevention measures, such as stone square and concrete fence, were used in a section of the Qinghai-Tibet Railway, and the investment of sand prevention work was from $1.95×10^6$ to $10.36×10^6$ CNY/km. In this study, the difference in the edge length between square and regular hexagonal sand barriers was analyzed using a mathematical model. Then, the costs of sand barriers made of various materials under a given area were compared. The results can provide a theoretical basis for an accurate estimation of material consumption of several common designs of sand barriers in desertified regions.

2　Study area

The study area was a desertified region (37°31′N, 105°09′E; 1100–2955 m a.s.l.) in the Shapotou area on the southeastern edge of the Tengger Desert, China. The landform of the study area can be

divided into five major units: desert, Yellow River alluvial plain, platform, mountain, and basin. The main landscape type of this area is sand dune, which belongs to the transition zone from desertification steppe to steppe desert (Li et al., 2014). The Tengger Desert is situated at the convergence of arid and semi-arid steppes. The climate is temperate, dry, and windy (Yang and Chongyi, 2010). The annual mean temperature is 7.0°C–9.7°C, with monthly means ranging from –6.7°C in January to 24.1°C in July (Wen and Dong, 2016). The Shapotou area receives an average of 186.0 mm precipitation annually. The annual average wind speed is 2.8 m/s, the maximum wind speed is 19.0 m/s, and the wind direction is mainly north-west (Xie et al., 2021).
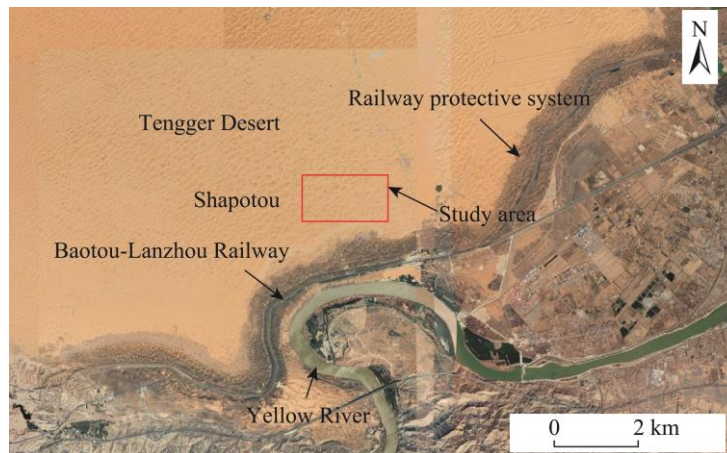

Fig. 1   Overview of the study area

3   Methodology

The principle of the mathematical model adopted is the grid division, primarily studying the method of discrete spatial data fields into simplex geometry (Zheng and Wu, 2005). An original land grid division model was used in this study, which refers to the modelling methods commonly utilized in the mathematical model of Chen (1995). The main steps of the model are dispersing a given area into a matrix of several small squares and then calculating the sum of the side lengths of the main and error areas. The side lengths of the two areas are solved separately.

3.1   Grid processing based on the square filling

When grids are used to divide a given area, the *xoy* plane rectangular coordinate system is established in the main area, as shown in Figure 2. The principle is as follows: for a given area A (m²), the lengths of the area are defined as the length l_x (m) in the *x*-direction and width l_y (m) in the *y*-direction. Then, it is discretized into a matrix of several small squares, where the side length of the small square is defined as a and the matrix is considered as the main area A_m (m²). The main area A_m may not be able to completely fill the given area, so the part to be filled is defined as the error area A_e (m²). Thus, the total area (A_T; m²) mesh division is the sum of the main and error areas. The grid division diagram is shown in Figure 2. The shaded part is the error area, arranged in the same way as the main area.

The maximum numbers of squares with the side length a that can be arranged in the *x*-direction and *y*-direction within the given area are calculated using the following equations:

$$n_x = \left[\frac{l_x}{a}\right], \tag{1}$$

$$n_y = \left[\frac{l_y}{a}\right], \tag{2}$$

where n_x and n_y are the maximum numbers of squares that can be accommodated in the *x*-direction and *y*-direction in a given area, respectively. Their values are the largest positive integers in the corresponding directions. Therefore, the main area is a matrix composed of $n_x \times n_y$ squares.
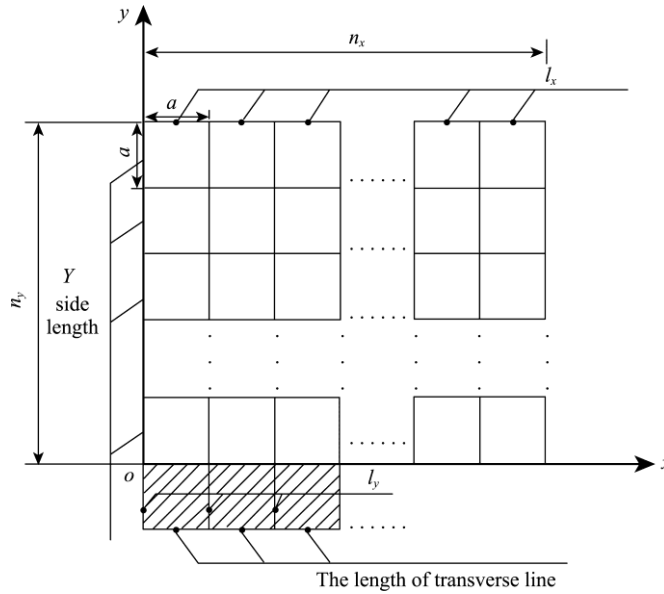

Fig. 2 Gridding diagram of square sand barriers analyzed in this study. *a*, the side length of the small square; n_x and n_y are the maximum numbers of squares that can be accommodated in the *x*-direction and *y*-direction in a given area, respectively; l_x, the length in the *x*-direction; l_y, the width in the *y*-direction.

A_m (m^2) is defined as the matrix of the main area, which can be calculated using the following equation:

$$A_m = n_x n_y a^2 . \tag{3}$$

For a given area A (m^2), n_e is defined as the number of squares to be filled in the error area and it can be calculated as:

$$n_e = \left[\frac{A - A_m}{a^2} \right] . \tag{4}$$

The area of the error region A_e (m^2) can be calculated using Equation 5:

$$A_e = n_e a^2 . \tag{5}$$

Thus, the actual total area A_T (m^2) can be calculated as:

$$A_T = A_m + A_e . \tag{6}$$

The given area is divided into the main and error areas, and the total edge length of the gridded graph can be solved. For the error area, the length of the side parallel to the *x*-direction is defined as the horizontal length, and the length parallel to the *y*-direction is defined as the vertical length.

The total side length of the gridded graph is the sum of the side lengths of the main and error areas, and the side lengths of the two areas are solved separately. Since the main body area is a matrix, the lengths in the *x*-direction and *y*-direction sides are expressed as D_x (m) and D_y (m), respectively:

$$D_x = n_x a(n_y + 1) , \tag{7}$$

$$D_y = n_y a(n_x + 1) . \tag{8}$$

As for the error area, the arrangement mode is still consistent with the main area, so the maximum number of lines that can be formed by the error area is N_e (number). The calculation

method is as follows:

$$N_e = \left\lceil \frac{n_e}{n_x} \right\rceil . \tag{9}$$

N_e takes the smallest positive integer greater than the calculated result. Therefore, the total side length of the error area (D_e; m) is calculated using Equation 10:

$$D_e = (2n_e + N_e)a . \tag{10}$$

The total side length of the gridded graph is defined as D (m). The calculation formula is as follows:

$$D = D_x + D_y + D_e = (2n_x n_y + n_x + n_y)a + (2n_e + N_e)a . \tag{11}$$

3.2 Grid processing based on the regular hexagonal filling

When the regular hexagon is used to grid a given area, the principle is the same as that of square division. For a given area S (m^2), the length of the area is defined as the length l_x (m) in the x-direction and width l_y (m) in the y-direction. It is discretized into a matrix of several regular hexagons, where the side length of the small regular hexagon is b (m), and the matrix is defined as the main area S_m (m^2). The main area S_m may fail to completely fill the given area, so the part to be filled is defined as the error area S_e (m^2). Thus, the total area S_T after the final mesh division is the sum of the main and error areas. The grid division diagram is shown in Figure 3. The shaded part is the error area, and the error area still adopts the arrangement mode of the main area.
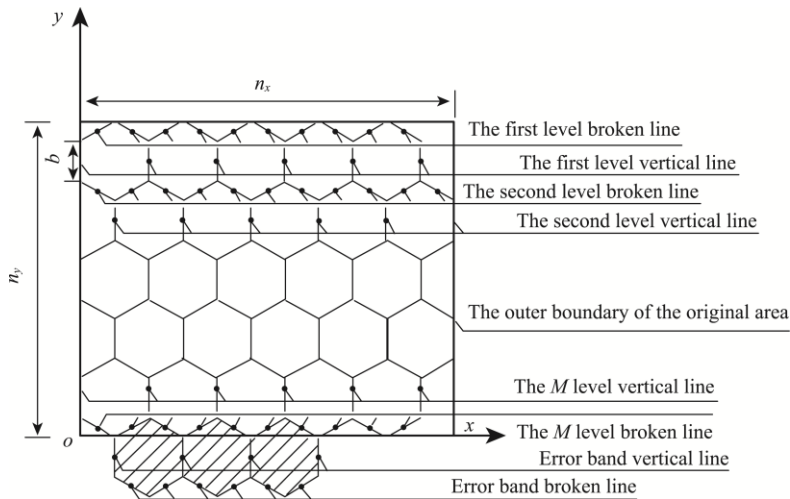

Fig. 3 Edge length solution diagram of the gridded graph. b, the side length of the small regular hexagons; M, the layer number of the line.

The maximum numbers of regular hexagons with the side length b (m) that can be arranged in the x-direction and y-direction within a given area are calculated as follows:

$$n_x = \left\lfloor \frac{2l_x - \sqrt{3}b}{2\sqrt{3}b} \right\rfloor , \tag{12}$$

$$n_y = \left\lfloor \frac{2l_y - b}{3b} \right\rfloor . \tag{13}$$

The values of n_x and n_y are the largest positive integers not exceeding the calculated results. Therefore, the main area is a matrix composed of $n_x \times n_y$ regular hexagons.

The main area (S_m; m^2) is calculated as follows:

$$S_m = \frac{3\sqrt{3}b^2}{2} n_x n_y . \tag{14}$$

Thus, the number of regular hexagons to be filled in the error area is defined as m_e, which can be calculated using Equation 15:

$$m_e = \left[\frac{2(S - S_m)}{3\sqrt{3}b^2} \right].$$ (15)

The error area (S_e; m^2) can be calculated as follows:

$$S_e = \frac{3\sqrt{3}b^2 m_e}{2}.$$ (16)

Therefore, the actual total area (S_T; m^2) is defined as follows:

$$S_T = S_m + S_e.$$ (17)

The given area is divided into the main and error areas, and the total edge length of the gridded graph can be calculated. In the process of solving the total edge length, the whole graph is divided into a set of broken and vertical lines. The total edge length of the graph is the sum of the main and error areas. When using regular hexagons to fill the body area, the side length is divided into two parts. The first part is the total length of the body area S_m and the second part is the hexagonal matrix composed of subject areas that do not completely fill the original area. The result is not included in the length of the outer boundary of the side length calculation. The specific definition is presented in Figure 3. The bold line refers to the outer boundary.

The total side length of the gridded graph is the sum of the side lengths of the main and error areas; thus, the side lengths of the two areas are solved separately.

Since the main area is a matrix, the total side length of hexagonal broken line (D_{mz}; m) and the total side length of hexagonal vertical line (D_{ms}; m) can be calculated using Equations 18 and 19, respectively:

$$D_{mz} = (2n_x n_y + n_y + 2n_x - 1)b,$$ (18)

$$D_{ms} = (n_x + 1)n_y b.$$ (19)

It should be noted that the main area is not included in the outer boundary of the calculation. The length of parallel x-axis boundary is defined as D_{cx} (m):

$$D_{cx} = l_x.$$ (20)

The boundary length parallel to the y-direction should be discussed separately. When $l_x = \sqrt{3}/2(2n_x + 1)$, a regular hexagon in the x-direction can fill the given area. D_{cy} (m) is the length of parallel y-axis boundary:

$$D_{cy} = 2l_y - n_y b.$$ (21)

When $l_x \neq \sqrt{3}/2(2n_x + 1)$, a regular hexagon in the x-direction cannot fill the given area.

The length of parallel y-axis boundary can be calculated as:

$$\begin{cases} D_{cy} = l_y + \dfrac{2n_y + 1}{2} \times b & n_y \rightarrow \text{even number} \\[3mm] D_{cy} = 2l_y - \dfrac{n_y + 1}{2} \times b & n_y \rightarrow \text{odd number} \end{cases}.$$ (22)

The part where the error area intersects with the peripheral boundary is not included in the calculation of the edge length.

Regarding the uniqueness of regular hexagonal shape arrangement, the error area should be discussed separately. Since the arrangement is still consistent with the main area, the maximum number of lines that can be formed by the error area should be determined first:

$$N_e = \left[\frac{m_e}{n_x} \right].$$ (23)

N_e takes the smallest positive integer greater than the calculated result.

When the number of filling grids in the last line of the error area is consistent with the length l_x

in the given area, that is, $m_e=n_xN_e$, then the broken line length of the error area (D_{ez}; m) and the vertical line length of the error area (D_{es}; m) can be obtained:

$$\begin{cases} D_{ez}=N_e b(2n_x +1) \\ D_{es}=(m_e + N_e)b \end{cases}. \tag{24}$$

However, when $m_e \neq n_xN_e$, the lengths of D_{ez} and D_{es} can be calculated as:

$$\begin{cases} D_{ez}=(2m_e + N_e -1)b \\ D_{es}=(m_e + N_e)b \end{cases}. \tag{25}$$

When the peripheral boundary is not considered, the total edge length of the gridded graph is:

$$D = D_{mz} + D_{ms} + D_{cx} + D_{cy} +D_{ez} + D_{es}. \tag{26}$$

3.3 Cost analysis method

This study referred to the material cost of sand barriers studied by various scholars and calculated the material cost and material utilization amount of square and regular hexagonal sand barriers with different materials (wheat straw, corn stalk, *S. mongolica*, poly lactic acid (PLA), magnesium cement, and high-density polyethylene (HDPE)) and varying sizes (1.0 m×1.0 m, 2.0 m×2.0 m, and 3.0 m×3.0 m). Zhang et al. (2019) stated that the material utilization amounts of square straw and corn stalk sand barriers are 0.53 and 0.59 kg/m, respectively. The material costs of square straw and corn stalk sand barriers are 0.90 and 0.65 CNY/kg, respectively. The total material costs of square straw and corn stalk sand barriers with the size of 2.0 m×2.0 m are 318.16 and 256.10 CNY/667.0 m², respectively. Dong et al. (2006) pointed out that the material cost of square *S. mongolica* sand barriers with the size of 1.0 m×1.0 m in the Tengger Desert and Hobq Desert highways is 7800.00 CNY/(hm²·a). The total material cost of *S. mongolica* sand barriers is 520.00 CNY/667.0 m². Tao et al. (2015) found that the material cost of *S. mongolica* sand barriers in an arid desert area of the lower reaches of Shiyang River is 7.50 CNY/kg, and the material utilization amount of *S. mongolica* in production is 1.17 kg/m², indicating that the total material cost of *S. mongolica* sand barriers is approximately 5830.00 CNY/667.0 m². It can be seen that the material costs of *S. mongolica* sand barriers varied significantly in these two studies. In this research, we adopted the data from the latter study, primarily for the following three reasons. First, the material cost in the study of Tao et al. (2015) is closer to the current price. Second, *S. mongolica* is mainly produced in Inner Mongolia Autonomous Region of China; it is often used as a local sand control material and the material cost is relatively low in the surrounding area. The sand control engineering project involved in Tao et al. (2015) is located in Gansu Province (adjacent to Inner Mongolia) and the price of *S. mongolica* is more universal. Last, based on the sand control engineering data (Tang, 2019), the material costs of *S. mongolica* sand barriers from Jiuquan to Ejin Railway section in Gansu and from Machanghao to Hejiata Railway section in Inner Mongolia are 6056.36 and 7030.18 CNY/667.0 m², respectively. The material costs are relatively close to those reported by Tao et al. (2015).

In this study, the material cost data of PLA, magnesium cement, and high-density polyethylene (HDPE) we collected from three sources: the sand control engineering project construction drawing files, the company's product quotation, and a related material website (https://b2b.baidu.com/land?id=2421830bef75e081452251ff00605c4810). The difference in material costs depends mainly on the origin, transportation cost, and project scale. Therefore, in order to make the material costs more representative, we used the real prices of the actual sand control engineering projects and the costs mentioned in the relevant literature of sand control engineering projects as the material cost data in this study. Further, the sale prices of companies selling sand control materials were collected through interviews.

3.4 Simulation scenarios

3.4.1 Grid processing of square filling

A simulated space with a length of 15.0 m, a width of 44.5 m, and an area of 667.5 m² was

divided into squares with the side lengths of 1.0, 2.0, and 3.0 m based on the field conditions (Fig. 4). The total side length of the gridded graph was then obtained.
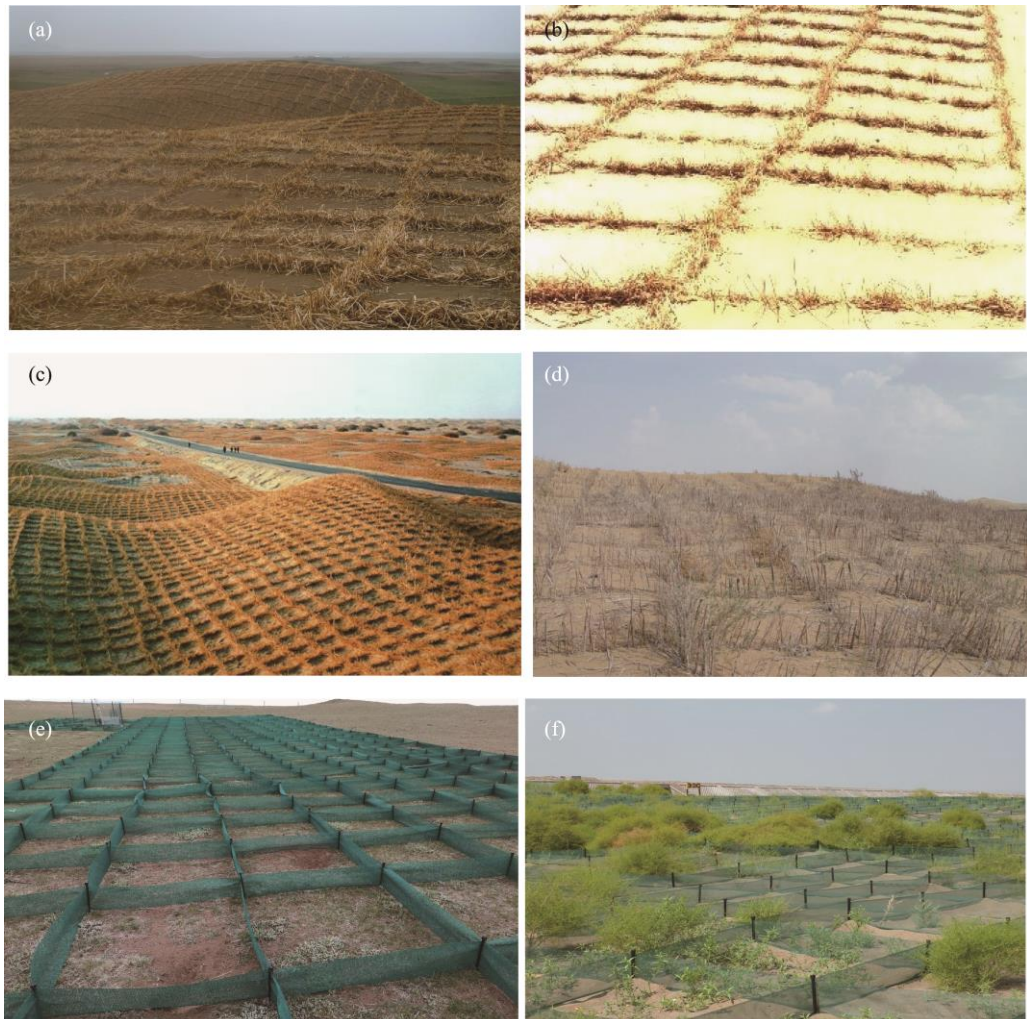

Fig. 4 Square sand barriers with various materials and sizes in different regions of China. (a), square straw sand barriers with the size of 1.0 m×1.0 m and the height of 20 cm in Zhongwei City, Ningxia Hui Autonomous Region; (b), square straw sand barriers with the size of 2.0 m×2.0 m and the height of 20 cm in the Shapotou area section of the Baotou-Lanzhou Railway; (c) square reed sand barriers with the size of 1.0 m×1.0 m and the height of 20 cm along the Taklimakan Desert Highway; (d), square *Salix Mongolica* sand barriers with the size of 1.5 m×1.5 m in the Shapotou area section of the Baotou-Lanzhou Railway; (e) polylactic acid (PLA) net sand barriers with the size of 1.0 m×1.0 m and the height of 20 cm in Maqu County, Gansu Province; (f), high-density polyethylene (HDPE) net sand barriers with the size of 1.0 m×1.0 m and the height of 20 cm in the section of the Lanzhou-Urumqi High-speed Railway.

3.4.2 Grid processing of regular hexagon filling

The land with a length of 15.0 m, a width of 44.5 m, and an area of 667.5 m^2 was divided into regular hexagons with the side lengths of 1.0, 2.0, and 3.0 m according to the field conditions (Fig. 5). The total side length of the gridded graph was then obtained.

4 Results

4.1 Cost of square filled sand barriers

Based on the above land grid division model for optimal resource utilization, we obtained the
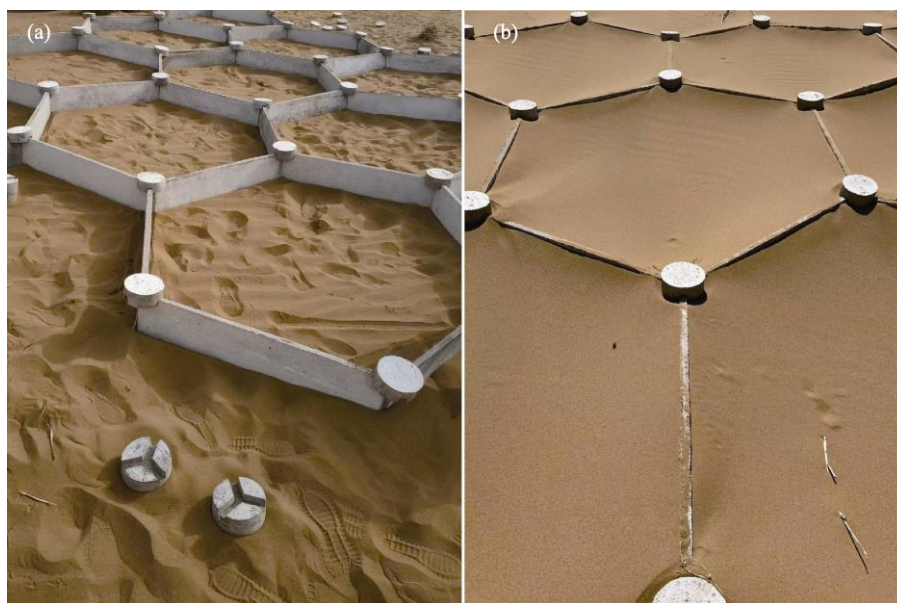
Fig. 5 Regular hexagonal magnesium cement sand barriers in the Shapotou area section of the Baotou-Lanzhou Railway. (a), regular hexagonal magnesium cement sand barriers with the size of 1.0 m×1.0 m and the height of 20 cm in the Shapotou area section of the Baotou-Lanzhou Railway before sand burial; (b) regular hexagonal magnesium cement sand barriers with the size of 1.0 m×1.0 m and the height of 20 cm in the Shapotou area section of the Baotou-Lanzhou Railway after sand burial.

results of the square filling, as shown in Figure 2. For the area with the length of 15.0 m, the width of 44.5 m, and the area of 667.5 m², the total side length of square sand barriers comprised D_x, D_y, and D_e. The total D_x side lengths of 1.0, 2.0, and 3.0 m square sand barriers are 675.0, 322.0, and 225.0 m, respectively. The total D_y side lengths of 1.0, 2.0, and 3.0 m square sand barriers are 704.0, 352.0, and 252.0 m, respectively. The total D_e side lengths of 1.0, 2.0, and 3.0 m square sand barriers are 15.0, 52.0, and 27.0 m, respectively. Therefore, the results of calculations with the side lengths of 1.0, 2.0, and 3.0 m are 1394.0, 726.0, and 504.0 m, respectively.

The total material costs of square wheat straw sand barriers for the three different types (side lengths of 1.0, 2.0, and 3.0 m) are 664.94, 346.30, and 240.41 CNY/667.0 m², respectively. The total material costs of square corn stalk sand barriers for the side lengths of 1.0, 2.0, and 3.0 m are 534.60, 278.42, 193.28 CNY/667.0 m², respectively. The total material cost of square *S. mongolica* sand barriers is approximately six times that of square corn stalk sand barriers for the same size. The total material costs of square PLA net sand barriers for the side lengths of 1.0, 2.0, and 3.0 m are 2790.00, 1452.00, and 1008.00 CNY/667.0 m², respectively. The total material cost of square HDPE net sand barriers is approximately 62% of the price of square PLA net sand barriers for the same size. Under the three different sand barrier sizes (1.0 m×1.0 m, 2.0 m×2.0 m, and 3.0 m×3.0 m), the material cost of square magnesium cement board sand barriers is approximately two times that of square PLA net sand barriers. Details are listed in Table 1.

4.2   Cost of regular hexagonal filled sand barriers

Based on the above land grid division model for optimal resource utilization, we obtained the results of the regular hexagonal filling, as shown in Figure 3. For the area with the length of 15.0 m, the width of 44.5 m, and the area of 667.5 m², the total side lengths of regular hexagonal sand barriers are composed of D_{mz}, D_{ms}, D_{cx}, D_{cy}, D_{ez}, and D_{es}. The total D_{mz} side lengths of 1.0, 2.0, and 3.0 m regular hexagonal sand barriers are 508.0, 206.0, and 144.0 m, respectively. The total D_{ms} side lengths of 1.0, 2.0, and 3.0 m regular hexagonal sand barriers are 261.0, 112.0, and 81.0 m, respectively. The total D_{cx} side lengths of 1.0, 2.0, and 3.0 m regular hexagonal sand

Table 1 Cost calculation results for different types of sand barriers

Sand barrier type	Size	Unit material utilization amount (kg/m)	Total length (m/667.0 m^2)	Total material utilization amount (kg/667.0 m^2)	Unit material cost (CNY/kg)	Total material cost (CNY/667.0 m^2)
Square wheat straw sand barrier	1.0 m×1.0 m	0.53	1394.0	738.82	0.90	664.94
	2.0 m×2.0 m	0.53	726.0	384.78	0.90	346.30
	3.0 m×3.0 m	0.53	504.0	267.12	0.90	240.41
Regular hexagonal wheat straw sand barrier	1.0 m×1.0 m	0.53	936.0	496.08	0.90	446.47
	2.0 m×2.0 m	0.53	568.5	301.31	0.90	271.18
	3.0 m×3.0 m	0.53	434.0	230.02	0.90	207.02
Square corn stalk sand barrier	1.0 m×1.0 m	0.59	1394.0	822.46	0.65	534.60
	2.0 m×2.0 m	0.59	726.0	428.34	0.65	278.42
	3.0 m×3.0 m	0.59	504.0	297.36	0.65	193.28
Regular hexagonal corn stalk sand barrier	1.0 m×1.0 m	0.59	936.0	552.24	0.65	358.96
	2.0 m×2.0 m	0.59	568.5	335.42	0.65	218.02
	3.0 m×3.0 m	0.59	434.0	256.06	0.65	166.44
Square *Salix Mongolica* sand barrier	1.0 m×1.0 m	0.30	1394.0	422.38	7.50	3167.85
	2.0 m×2.0 m	0.30	726.0	220.00	7.50	1650.00
	3.0 m×3.0 m	0.30	504.0	152.71	7.50	1145.33
Regular hexagonal *S. mongolica* sand barrier	1.0 m×1.0 m	0.30	936.0	283.61	7.50	2127.08
	2.0 m×2.0 m	0.30	568.5	172.26	7.50	1291.95
	3.0 m×3.0 m	0.30	434.0	131.50	7.50	986.25
Square PLA net sand barrier	1.0 m×1.0 m	0.02	1394.0	27.90	100.00	2790.00
	2.0 m×2.0 m	0.02	726.0	14.52	100.00	1452.00
	3.0 m×3.0 m	0.02	504.0	10.08	100.00	1008.00
Regular hexagonal PLA net sand barrier	1.0 m×1.0 m	0.02	936.0	18.72	100.00	1872.00
	2.0 m×2.0 m	0.02	568.5	11.37	100.00	1137.00
	3.0 m×3.0 m	0.02	434.0	8.68	100.00	868.00
Square HDPE net sand barrier	1.0 m×1.0 m	0.03	1394.0	34.85	50.00	1742.50
	2.0 m×2.0 m	0.03	726.0	18.15	50.00	907.50
	3.0 m×3.0 m	0.03	504.0	12.60	50.00	630.00
Regular hexagonal HDPE net sand barrier	1.0 m×1.0 m	0.03	936.0	23.40	50.00	1170.00
	2.0 m×2.0 m	0.03	568.5	14.21	50.00	710.50
	3.0 m×3.0 m	0.03	434.0	10.85	50.00	542.50
Regular hexagonal magnesium cement board sand barrier	1.0 m×1.0 m	10.00	1394.0	13,940.00	0.40	5576.00
	2.0 m×2.0 m	10.00	726.0	7260.00	0.40	2904.00
	3.0 m×3.0 m	10.00	504.0	5040.00	0.40	2016.00
Regular hexagonal magnesium cement board sand barrier	1.0 m×1.0 m	10.00	936.0	9360.00	0.40	3744.00
	2.0 m×2.0 m	10.00	568.5	5685.00	0.40	2274.00
	3.0 m×3.0 m	10.00	434.0	4340.00	0.40	1736.00

Note: PLA, poly lactic acid; HDPE, high-density polyethylene.

barriers are all 15.0 m. The total D_{cy} side lengths of 1.0, 2.0, and 3.0 m regular hexagonal sand barriers are 74.0, 73.5, and 74.0 m, respectively. The total D_{ez} side lengths of 1.0, 2.0, and 3.0 mregular hexagonal sand barriers are 51.0, 102.0, and 75.0 m, respectively. The total D_{es} side lengths of 1.0, 2.0, and 3.0 m regular hexagonal sand barriers are 27.0, 60.0, and 45.0 m,

respectively. The results of calculations for the area with the side lengths of 1.0, 2.0, and 3.0 m are 936.0, 568.5, and 434.0 m, respectively.

The total material costs of regular hexagonal wheat straw sand barriers for the three different types (the side lengths of 1.0, 2.0, and 3.0 m) are 446.47, 271.18, and 207.02 CNY/667.0 m², respectively. The total material costs of regular hexagonal corn stalk sand barriers for the side lengths of 1.0, 2.0, and 3.0 m are 358.96, 218.02, and 166.44 CNY/667.0 m², respectively. The total material costs of regular hexagonal *S. mongolica* sand barriers for the side lengths of 1.0, 2.0, and 3.0 m are 2127.08, 1291.95, and 986.25 CNY/667.0 m², respectively. The total material costs of regular hexagonal PLA net sand barriers for the side lengths of 1.0, 2.0, and 3.0 m are 1872.00, 1132.00, and 868.00 CNY/667.0 m², respectively. The total material cost of regular hexagonal HDPE net sand barriers is approximately 63% that of regular hexagonal PLA net sand barriers for the same size. Under the three different sand barrier sizes (1.0 m×1.0 m, 2.0 m×2.0 m, and 3.0 m×3.0 m), the material cost of regular hexagonal magnesium cement board sand barriers is approximately two times that of regular hexagonal PLA net sand barriers.

5 Discussion

5.1 Barrier costs

The selection of sand barrier materials should comprehensively consider the cost, benefit of windbreak, and sand fixation effect. Wheat straw, corn stalk, and *S. mongolica* are widely used in desertification control as common sand barrier materials (Guo et al., 2004; Meng et al., 2010; Wang et al., 2020). In terms of cost, corn stalk has a lower price and a longer protection time than other materials (Zhang et al., 2019). This study estimated the material costs of square and regular hexagonal corn stalk sand barriers with the sizes of 2.0 m×2.0 m and 3.0 m×3.0 m using a mathematical model, and the results showed that the material cost of regular hexagonal corn stalk sand barriers with the size of 3.0 m×3.0 m is the lowest. Using a land grid division model for optimal resource utilization, we calculated that the total material costs of square wheat straw and corn stalk sand barriers with the size of 2.0 m×2.0 m are 346.30 and 278.42 CNY/667.0 m², respectively. These results are slightly higher than those of Zhang et al. (2019). The reason for the discrepancy is that different total side lengths in the same area can lead to the difference of material cost. Additionally, when the total area is fixed, the total side lengths of square and regular hexagonal sand barriers were compared under the sizes of 1.0 m×1.0 m, 2.0 m×2.0 m, and 3.0 m×3.0 m. The total side lengths of square sand barriers are 458.0, 157.5, and 70.0 m higher than the total side lengths of regular hexagonal sand barriers for the three types of sizes, respectively. For the size of 1.0 m×1.0 m, square and regular hexagonal sand barriers have the largest difference in the edge length, and the cost-saving effect is remarkable compared with other sizes. Moreover, by comparing the wheat straw and corn stalk materials, although the unit utilization amount of corn stalk is higher than that of wheat straw, the cost of corn stalk material is relatively low. The total cost of corn stalk material is lower than that of wheat straw material for the three sizes of sand barriers (1.0 m×1.0 m, 2.0 m×2.0 m, and 3.0 m×3.0 m). Furthermore, by comparing the two different division methods, the regular hexagonal corn stalk sand barrier has an evident price advantage over an area of approximately 667.0 m². For the commonly used 1.0 m×1.0 m size sand barrier, the total material cost of regular hexagonal corn stalk sand barriers accounts for approximately 54% of the total material cost of square wheat straw sand barriers.

It is not enough to discuss the cost of sand barriers from the perspective of material cost alone because the price depends on the environment, wind strength, transportation cost, service life, and other influencing factors. Therefore, the issue on the cost of sand barriers needs to be discussed separately. The material costs of corn stalk and wheat straw sand barriers are low, but their service life is relatively short, typically 1.5–3.0 a (Dong et al., 2006). Therefore, corn stalk and wheat straw sand barriers are suitable for desert areas with annual precipitation of more than 200.0 mm and low degree of wind-blown sand. The reason for this is that vegetation can recover quickly

during the service life of these barriers. These two kinds of sand barriers (corn stalk and wheat straw) can not only ensure windbreak and sand fixation, but also maximize cost savings and apply to mechanization (Ding, 2022). Transportation costs can be further reduced, particularly in the northwest of China, where corn and wheat grass can be grown locally.

Although the cost of *S. mongolica* material is higher than that of other materials, the service life of *S. mongolica* is longer than 5.0 a. By comprehensive comparison, the annual operating cost of regular hexagonal *S. mongolica* sand barriers with the size of 3.0 m×3.0 m is lower than that of square corn stalk sand barriers with the size of 1.0 m×1.0 m, at values of 197.30 and 267.30 CNY/667.0 m^2, respectively. Additionally, the price and transportation cost of *S. mongolica* material is relatively low. Therefore, *S. mongolica* can be used as the main sand barrier material for windbreak and sand-fixation projects in Inner Mongolia. Song (2011) indicated that *S. mongolica* sand barriers with the size of 2.0 m×4.0 m can also contribute to sand erosion prevention. Our results demonstrated that *S. mongolica* sand barriers with the sizes of 2.0 m×2.0 m and 3.0 m×3.0 m can be used to further reduce costs without affecting the windbreak and sand fixation effects in practice.

The biggest advantages of HDPE and PLA materials are good abrasion resistance and long service life. Hong et al. (2020) and Qu et al. (2021) stated that the service life of HDPE material is longer than 5.0 a and that of PLA material is longer than 3.0 a. Under the same sand barrier size, the annual operating cost of HDPE net sand barriers is lower than that of corn stalk sand barriers. Therefore, HDPE and PLA net sand barriers are suitable for areas with long sand control period, lack of other sand barrier materials, and low annual precipitation, such as the Tibetan region. Moreover, these two materials can be mechanically operated during construction and recycled once the vegetation is restored. These materials have the potential to further reduce cost in future applications and practices. The selection of sand barrier types should comprehensively consider the cost of materials, environment, sand fixation benefit, and service life. It is an important way to control the cost of sand barriers to choose appropriate materials according to local conditions.

5.2　Barrier materials

The branches of *S. mongolica* can survive in harsh natural environment, with the effects of windbreak and sand fixation. Therefore, the establishment of *S. mongolica* sand barriers can achieve the dual objectives of engineering sand control and biological sand control (Gao et al., 2004). *S. mongolica* can be set into solid sand barriers through mechanical operation, which is more convenient (Gao et al., 2013). Liu et al. (2021b) proposed that the transition rate of aeolian sand is positively correlated with reed height and negatively correlated with grass square spacing, and suggested that from the aspect of sand fixation effect, the optimal design of grass checkerboard sand barriers in the desert areas in the south of Xinjiang is as follows: the reed height of 20 cm and the grass checkerboard size of 1.0 m×1.0 m. Recently, new materials for sand fixation barriers resembling grass squares are emerging, such as PLA material, which can be made into regular hexagonal sand barriers and further improve the windbreak and sand fixation while meeting the cost conditions. Liu et al. (2019) studied the windbreak and sand fixation effects of sand barriers with varying geometric shapes and materials by comparing the surface roughness, windbreaking efficiency, and wind speed of sand barriers. Their results revealed that compared with straw sand barriers, PLA net sand barriers can effectively increase the surface roughness and improve the windbreak efficiency while reducing the surface wind speed and decreasing the surface sediment transport.

Sun et al. (2017) stated that the wind proofing efficiency of regular hexagonal sand barriers with the size of 1.0 m×1.0 m is significantly higher than that of square sand barriers with the size of 1.0 m×1.0 m. The wind proofing efficiency of regular hexagonal sand barriers is 8% higher than that of square sand barriers at 0.2 m height above the ground and 10% higher at 0.3 m height above the ground. Zhang et al. (2016) found that the surface roughness of regular hexagonal sand

barriers is larger than that of square sand barriers. Under the influence of sand barriers, the surface roughness increases rapidly with the increasing in wind speed under low wind speed conditions. When the wind speed is greater than 7.0 m/s, the increase in the rate of the surface roughness decreases greatly. Regular hexagonal sand barriers have evident advantages over square sand barriers in sand fixation efficiency.

6 Conclusions

Based on the land grid division model for optimal resource utilization, this study calculated the side length differences between square and regular hexagonal sand barriers with different sizes, and evaluated the material cost and material utilization amount of sand barrier with different materials and sizes. The material cost of different sizes of sand barriers under different grid division standards was then calculated by combining the side length. Comprehensive comparison of material costs of wheat straw, corn stalk, *S. mongolica*, PLA, magnesium cement, and HDPE net sand barriers with the size of 1.0 m×1.0 m showed that corn stalk has the lowest material cost, followed by wheat straw, HDPE, PLA, *S. mongolica*, and magnesium cement. Similarly, the material cost of regular hexagonal corn stalk sand barriers with the size of 3.0 m×3.0 m is the lowest, while the material cost of square magnesium cement board sand barriers with the size of 1.0 m×1.0 m is the highest. The material cost of regular hexagonal sand barriers is lower than that of square sand barriers with the same size and material. When considering the lowest total sand barrier cost, regular hexagonal corn stalk sand barriers with the size of 3.0 m×3.0 m should be considered first in areas with annual precipitation of higher than 200.0 mm. However, when considering the effects of the environment, wind speed, transportation cost, service life, and other influencing factors on the cost of sand barriers, regular hexagonal *S. mongolica* sand barriers with the size of 2.0 m×2.0 m or 3.0 m×3.0 m should be selected in desertified regions of Inner Mongolia. Further, regular hexagonal HDPE net sand barriers with the size of 3.0 m×3.0 m should be considered in areas with little precipitation and lack of sand barrier materials. Mechanical operation provides strong support for the construction of regular hexagonal sand barriers. Therefore, the installation of sand barriers can be reasonably planned according to the protection requirements and budget.

Acknowledgements

References

Chen Y H. 1995. Mathematical Model. Chongqing: Chongqing University Press, 13–16. (in Chinese)

Cheng C C, Yan D R, Jiang H T, et al. 2014. Effects of sandbag sand barrier on soil hardness. Environmental Engineering, 864–867: 2623–2631.

Ding G D, Zhao T N, Fan J Y, et al. 2004. Review on the research status of desertification evaluation index system. Journal of Beijing Forestry University, 26(1): 92–96. (in Chinese)

Ding Y L. 2022. The applicability of different types of sand barriers. China Resources Comprehensive Utilization, 40(6): 27–32. (in Chinese)

Dong Z, Li H L, Hu C Y, et al. 2006. Comparative study on the benefit and cost of different sand fixation measures in desert highway. Research of Soil and Water Conservation, 13(2): 128–130. (in Chinese)

Gao Y, Qiu G Y, Ding G D, et al. 2004. Study on windbreak and sand-fixation efficiency of *Salix Mongolica* sand barrier. Journal of Desert Research, 24(3): 365–370. (in Chinese)

Gao Y, Yu Y, Gong P, et al. 2013. Study on Sand Barrier of *Salix Mongolica*. Beijing: Science Press, 55–60. (in Chinese)

Guo Y Q, Lee I B, Shimizu H, et al. 2004. Principles of sand dune fixation with straw checkerboard technology and its effects on the environment. Journal of Arid Environments, 56(3): 449–464.

Hong X L, Qu J J, Zhang J Q, et al. 2020. Service life evaluation of high density polyethylene (HDPE) sand control net. Journal of Desert Research, 40(3): 1–6. (in Chinese)

Jiang R C. 2020. Analysis on the application of straw checkerboard sand barrier in windbreak and sand fixation. Research on Agricultural Disaster, 10(9): 126–127. (in Chinese)

Jing M, Li Q, Zhang H, et al. 2022. Review on desertification control. Cooperative Economy and Technology, (6): 42–43. (in Chinese)

Lu L Q, Cui X X, Gao Y, et al. 2020. Comparison of windproof efficiency of different sand barriers made from sunflower straw and corn straw. Chinese Journal of Soil Science, 51(05): 1218–1223. (in Chinese)

Li C J, Wang Y D, Lei J Q, et al. 2021. Damage by wind-blown sand and its control measures along the Taklimakan Desert Highway in China. Journal of Arid Land, 13(1): 98–106. (in Chinese)

Li X R, Zhang Z S, Tan H J, et al. 2014. Ecological reconstruction and restoration of aeolian sand hazardous areas in northern China: discussion on soil moisture and vegetation carrying capacity in Tengger Desert. Science China Life Sciences, 44(3): 257–266. (in Chinese)

Ling Y Q. 1980. Protection Benefit of Grassy Checkered Sand Barrier. Yinchuan: Ningxia People's Publishing House, 49–59. (in Chinese)

Liu J, Nie H F, Xiao C, et al. 2021a. Desertification change in Northern China from 2010 to 2018. China Geological Survey, 8(6): 25–34. (in Chinese)

Liu J, Xiao Y P, Yu S H, et al. 2021b. Study on grass square barrier height and spacing of sediment and sand-fixation. The Western Traffic Science and Technology, 11: 203–205. (in Chinese)

Liu X J. 2019. Study on the effect of geometric shape on wind protection and sand fixation effects of two kinds of sand barriers. MSc Thesis. Hohhot: Inner Mongolia Agricultural University, 6–7. (in Chinese)

Meng L, Xin Y, Zha Y S. 2010. Influence of Horqin sandy land plant sand barrier on soil moisture. Advanced Materials Research, 113–116: 1110–1114.

National Forestry and Grassland Administration. 2015. The Fifth Bulletin on Desertification and Desertification in China. [2022-04-13]. http://www.forestry.gov.cn/. (in Chinese)

Qu J J, Hong X L, Li F, et al. 2021. Aging resistance and sand control effect of polylactic acid (PLA) grid sand barrier. Journal of Desert Research, 41(2): 51–58. (in Chinese)

Song H Y. 2011. Analysis of windbreak and sand fixation efficiency of *Salix Mongolica* sand barrier in Yulin. Shaanxi Forestry Science and Technology, (3): 23–25. (in Chinese)

Sun H, Liu J H, Huang Q Q, et al. 2017. Study on windproof effect of polygon grass sand barrier. Journal of Beijing Forestry University, 39(10): 90–94. (in Chinese)

Tao H X, Zhang X L, Gao C B. 2015. Integration of sand barrier installation technology and sand blocking effect in arid desert area of the lower reaches of Shiyang River. Gansu Technology, 31(17): 44–48. (in Chinese)

Wang D Q. 2012. Preliminary analysis of railway sandstorm control project investment. Journal of Railway Standard Design, (6): 21–24. (in Chinese)

Wang R, Dang X, Gao Y, et al. 2020. Alternated desorption-absorption accelerated aging of *Salix psammophila* sand barrier. BioResources, 15(3): 6696–6713.

Wang X Q, Lu Q, Yang H H, et al. 2009. Alpine sandy sand-fixation efficiency and ecological function in sandy observational studies. Journal of Soil and Water Conservation, 23(3): 38–41. (in Chinese)

Wang Y M. 2018. Effects of sand-fixing barriers on vegetation soil and biological soil crusts. MSc Thesis. Xi'an: Northwest University, 18–35. (in Chinese)

Wang Y M, Liu K, Qu J J. 2019. Effects of sand barriers on vegetation and soil nutrients in shifting sandy land. Journal of Desert Research, 39(3): 56–65. (in Chinese)

Wang Z T, Zheng X J. 2002. A simple model for size analysis of grassy checkered sand barrier. Journal of Desert Research, 22(3): 229–232. (in Chinese)

Wen Q, Dong Z. 2016. Geomorphologic patterns of dune networks in the Tengger Desert, China. Journal of Arid Land, 8(5): 660–669.

Wu Z. 2010. Aeolian Geomorphology and Sand Control Engineering. Beijing: Science Press, 310–330. (in Chinese)

Xie T, Li Y F, Li X J. 2021. Characteristics of soil crust and organic carbon mineralization in subsoil of sand-fixing vegetation area in southeastern margin of Tengger Desert. Ecological Acta, 41(6): 2339–2348. (in Chinese)

Xu L S, Xu X W. 1996. Study on sand-fixing engineering and ecological benefit of sand-barrier forest. Journal of Desert Research, 16(4): 392–396. (in Chinese)

Yang F M, Chongyi E. 2010. Correlation analysis between sand-dust events and meteorological factors in Shapotou, Northern China. Environmental Earth Sciences, 59(6): 1359–1365.

Yang Z. 2021. China's Rubik's Cube has been upgraded with a new grass-checkerboard sand barrier in Zhongwei Desert. [2022-04-23]. https://t.ynet.cn/baijia/30688761.html. (in Chinese)

Zhang C L, Li Q, Zhou N, et al. 2016. Field observations of wind profiles and sand fluxes above the windward slope of a sand dune before and after the establishment of semi-buried straw checkerboard barriers. Aeolian Research, 20: 59–70.

Zhang J, Liu W, Zhang Q D, et al. 2019. Study on the cost accounting of sand barrier installation and the effect of resistance of sand vegetation recovery. Journal of Forestry Science and Technology Communication, (11): 75–78. (in Chinese)

Zhang S S, Liu Z M, Yan Q L. 2009. Effects of sand barrier near interdune lowlands on the vegetation restoration of mobile sand dunes. Chinese Journal of Ecology, 28(12): 2403–2409. (in Chinese)

Zheng M, Wu L J. 2005. The method of arbitrary region meshing classification. Journal of Shenyang Normal University (Natural Science), 23(4): 32–35. (in Chinese)

Zhu Z D, Zhao X L, Ling Y Q, et al. 1998. Sand Control Engineering. Beijing: China Environmental Science Press, 55–78. (in Chinese)

chinaXiv:202210.00109v1